論 文 の 内 容 の 要 旨

応用生命工学　専攻
平成24年度博士課程　進学
氏　名　　南　煐　祐
指導教員名　　伏信　進矢

論文題目

Studies on structures of novel sugar metabolic enzymes

（新規な糖代謝経路で働く酵素の構造生物学的研究）

Living cells generally have sugar metabolic pathways for energy production, storage, maintenance of homeostasis, and creation of new biomolecules by catabolism and anabolism. The sugar metabolic pathways consist of sequential actions of various enzymes, such as hydrolases, oxidoreductases, transferases, lyases, or isomerases. The investigations of functional and structural properties for novel enzymes contribute to understand reaction mechanisms and to discover new sugar metabolic pathways. Glycolysis, the major pathway of carbohydrate metabolism, has evolved to process mainly the hexose monosaccharide glucose. Many of the enzymes in glycolytic pathways do not process other sugars because it is specialized for glucose. Thus, microorganisms have advanced alternative pathways linked to glycolysis to utilize other sugars. I studied enzymes in two novel alternative sugar metabolic pathways from microbes; intracellular pathways linked to oxidative cellulose degradation and bifidobacterial consumption of human milk oligosaccharides and intestinal mucin glycoproteins.

The extracellular hydrolytic enzymes involved in the oxidative cellulose degradation have been well studied. The recent discovery of lytic polysaccharide monooxygenases (LPMOs), which catalyze oxidative cleavage of cellulose chains, has changed the paradigm of cellulase research. LPMO, cellobiohydrolases, endoglucanases, and cellobiose dehydrogenase synergistically act on cellulose to produce mainly cellobionolactone, but it has been unknown how the product is further metabolized. More recently, a new intracellular enzyme cellobionic acid phosphorylase (CBAP, EC 2.4.1.321) that cleaves the non-enzymatically hydrolyzed aldonic acid compound of cellobionolactone was found from three cellulolytic microbes; the plant pathogenic bacterium *Xanthomonas campestris*, the red bread mold *Neurospora crassa*, and the marine bacterium *Saccharophagus degradans*. CBAP catalyzes reversible phosphorolysis of cellobionic acid (CbA) into α-D-glucose 1-phosphate (αG1P) and gluconic acid (GlcA). Molecular characterization of CBAPs contributes to understand the “missing link” between the oxidative cellulose degradation and the downstream glycolytic pathway.

The galacto-*N*-biose (GNB, Gal-β1,3-GalNAc)/lacto-*N*-biose I (LNB, Gal-β1,3-GlcNAc) pathway is a unique pathway found in infant gut-associated bifidobacteria to metabolize the degradation products of human milk oligosaccharides (LNB) and intestinal mucin glycans (GNB). The GNB/LNB pathway consists of three intracellular enzymes, and two of them (UDP-glucose hexose 1-phosphate uridylyltransferase as GalT and UDP-galactose 4-epimerase as GalE) are homologue enzymes of those in Leloir pathway, which is a well-studied galactose-metabolizing pathway. A notable feature of GalE and GalT in the GNB/LNB pathway is their wide substrate specificities that they can catalyze reactions using UDP-GalNAc/GlcNAc in addition to UDP-Gal/Glc. I studied the structural features, structural basis of substrate specificity and reaction mechanisms of these enzymes. Studies of these two sugar metabolic enzymes provide beneficial tools in the investigations of relationship between structure and function of enzymes for oligosaccharide synthesis, and for wide range of applications in biomass utilization and development of novel functional food for human health.

X-ray crystallography of CBAP involved in oxidative cellulose degradation pathway

I conducted crystallization screening of CBAPs from the three microbes. X-ray crystallography of CBAP from *S. degradans* was successfully done and described in chapter 2. Although CBAPs are classified into glycoside hydrolase (GH) family 94 along with cellobiose phosphorylase (CBP) and chitobiose phosphorylase (ChBP), molecular replacement using their structures was not successful due to low amino acid sequence similarity. The structure of CBAP was solved by single-wavelength anomalous dispersion method using selenomethionine-labeled protein, and an Apo form, and complex forms with CbA and GlcA were determined at 2.1, 1.6, 1.75 Å resolution, respectively. In the reverse reaction, CBAP synthesizes cellobionic acid (CbA) from GlcA as the acceptor in the presence of αG1P as the donor. CBAP also catalyzes the synthetic reaction using an alternative uronic acid acceptor, D-glucuronic acid (GlcUA), to produce 3-*O*-*β*-D-glucopyranosyl-D-glucuronic acid (Glc-*β*-1,3-GlcUA). Therefore, I also determined a complex structure with Glc-*β*-1,3-GlcUA at 1.8 Å resolution.

CBAP forms a tight homodimer in the crystal as well as in solution, and the overall structure was basically similar to those of other GH94 enzymes. The crystals were grown in in the presence of a high concentration of ammonium sulfate, and the phosphate binding site was occupied by a sulfate ion in all CBAP structures. In the CbA complex, the glucose and the GlcA moieties were bound at subsites –1 and +1, respectively, exhibiting a catalytically plausible structure for the phosphorolytic reaction (Fig. 1A). The C1 carboxyl group of the GlcA moiety of CbA interacts with R609 and K613. In the GlcA complex, a dehydrated compound glucono 1,5-lactone (LGC) and GlcA were bound at subsites –1 and +1, respectively. At subsite +1, the C1 carboxyl group of the GlcA interacts with R609, K613, and Q190' (from a neighboring molecule of the homodimer), suggesting that they are key residues for the molecular recognition of the aldonic acid. In the Glc-*β*-1,3-GlcUA complex, the GlcUA moiety was in a pyranose form and bound at a displaced position, and the C6 carboxyl group

does not interact with R609, K613, and Q190' (Fig. 1B). Instead, the anion binding site is occupied by a second sulfate ion.

To examine the importance of these residues on binding of the aldonic acid and the uronic acid, I conducted a mutational analysis. As expected, R609A and K613A showed almost undetectable activity for the synthetic reaction using GlcA, and Q190A showed significantly decreased activity (270-fold reduction of k_{cat}/K_m). Unexpectedly, R609A and K613A did not exhibit detectable activity also for GlcUA, and the Q190A mutation decreased the k_{cat}/K_m by 22-fold, indicating that these residues are also important for the uronic acid. Accorting to the result of mutants, I concluded that the Glc-β1,3-GlcUA complex was an artificial structure due to the high concentration of sulfate ion compared to the concentration of the disaccharide ligand used for the soaking experiment (10 mM). For the CbA and GlcA complex, the crystals were soaked in higher concentrations of the ligands (50 mM). I examined a possible binding mode of GlcUA at subsite +1 and confirmed that it can bind at a similar position to GlcA, placing its C6 carboxyl group at the site surrounded by R609, K613, and Q190'.

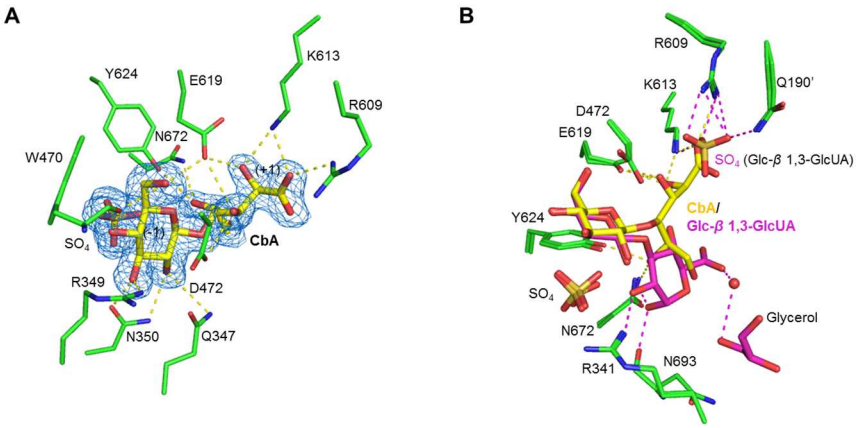

Figure. 1 Active site of CBAP in complex with cellobionic acid (A) and Glc-β 1,3-GlcUA (B).

In the amino acid-based sequence alignment, the residues recognizing GlcA at subsite +1 are not conserved in other GH94 enzymes whereas they are completely conserved in the three CBAPs. In a structural superimposition with GH94 CBP, the residues at subsite −1 are highly conserved but those at subsite +1 are completely different. In conclusion, it was revealed that CBAPs have a unique subsite +1 in the aspect of substrate specificity.

X-ray crystallography of GalE and GalT from *Bifidobacterium logum* involved in the GNB/LNB pathway

I conducted crystallization screening of GalE and GalT from *B. logum* (bGalE and bGalT, respectively). A preliminary structure of bGalT was solved at 2.4 Å resolution by a molecular replacement method, but crystallographic refinement is not sufficiently done yet. In chapter 3, I mainly describe about X-ray crystallography of bGalE focusing on its wide substrate specificity. GalE

from *Escherichia coli* (eGalE) has been extensively studied and catalyzes only the conversion between UDP-Gal and UDP-Glc. On the other hand, human GalE (hGalE) shows wide substrate specificity similar to bGalE, catalyzing the conversion of both UDP-Gal/Glc and UDP-GalNAc/GlcNAc.

The structures of bGalT in complex with UDP, UDP-Glc, and UDP-GlcNAc were determined at 1.8, 1.8, and 2.0 Å, respectively. The overall protein structure can be roughly divided into an NAD^+ binding N-terminal domain and an UDP-hexose binding C-terminal domain. The cofactor NAD^+ was intrinsically bound to all complexes. The nicotinamide ring of the NAD^+ took the *syn*-conformation with its *si*-face oriented toward the sugar ligands, and residues D32-S37 in NAD binding loop recognize the adenine ribose moiety. The distance between the sugar C4 atom of UDP-hexose and the nicotinamide ring C4 atom of NAD^+ was less than 3.4 Å in the UDP-hexose complex structures, suggesting that they are catalytically competent structures. In structural superimposition between UDP-Glc and UDP-GlcNAc complex, the side chain conformation of N200 at the UDP-hexose binding site was different; it swings "in" and "out" in the UDP-Glc and UDP-GlcNAc complex structures, respectively. The binding mode of UDP-GlcNAc in bGalE was similar to that of hGalE (Fig. 2A). For the catalysis of GalEs, the hexose moiety must rotate to adopt two different orientations, placing the C4 hydrogen atom of *galacto*- or *gluco*- hexoses toward the nicotinamide C4 atom of NAD^+ for a hydride transfer. As shown in Fig. 2, the hexose moiety of bGalE structure was in a similar orientation to those of hGalE and eGalE. The *N*-acetyl group in this orientation was accommodated by the swing of asparagine side chain (Fig. 2B). GalE with wide substrate specificity (bGalE and hGalE) has a small side chain residue (C299 and C307) at a potential site for the *N*-acetyl group in a flipped orientation. In contrast, eGalE has a large side chain residue (Y299) at this site and blocks binding of UDP-GlcNAc or UDP-GalNAc in the flipped orientation. Therefore, it was shown that the substrate specificity of GalE is primarily controlled by the side chain size at this residue.

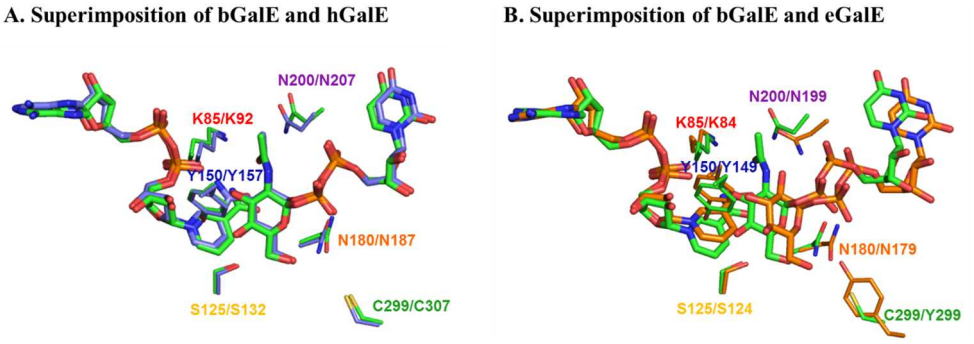

Figure 2 Substrate binding pocket of GlaE proteins.